Apparent slip over a solid-liquid interface with a no-slip boundary condition

Junfeng Zhang and Daniel Y. Kwok*

Nanoscale Technology and Engineering Laboratory, Department of Mechanical Engineering, University of Alberta, Edmonton, Alberta, Canada T6G 2G8

We studied solid-liquid slip by a mean-field free-energy lattice Boltzmann approach recently proposed [Phys. Rev. E **69**, 032602 (2004)]. With a general bounce-back no-slip boundary condition applied to the interface, liquid slip was observed because of the specific solid-fluid interactions. Our work relates interfacial slip to a more realistic solid-fluid interaction and hence contact angle. The kinetic nature of LBM is manifested in this interfacial study. A small negative slip length can also be produced with a stronger solid-fluid attraction.

In fluid mechanics, the no-slip boundary condition (BC) between a fluid and a solid surface has traditionally been an assumption in solving the governing Navier-Stokes (NS) equations [1]. Despite macroscopic experimental supports, it still remains an assumption without physical principles. In fact, studies on fluid slip has long been an interesting subject since the pioneering work by Navier [2] and Maxwell [3]. Recent measurements, however, indicate significant slip on solid surfaces [4–8]. Due to the difficulties in direct microscopic observation near the solid-fluid interface, molecular dynamics (MD) simulations have been widely used to study the relationship between fluid slip and the properties of fluid and solid [9–12]. In general, both experimental and MD simulation results show that there is a strong relationship between the magnitude of slip and the solid-fluid interaction: the weaker the interaction, the larger is the contact angle and hence the slip.

Recently, a mesoscopic approach, the lattice Boltzmann method (LBM) has experienced tremendous development in simulating fluid behaviors [13–16]. In bulk fluid, LBM is in fact a NS solver; however, at the solid-fluid interface, the kinetic nature of this method becomes manifest, because boundary conditions (BC's) are imposed on particle distributions rather than directly on fluid quantities such as velocity [17]. Succi [17] recently applied the LBM to study fluid slip on solid surfaces by employing a mix of bounce-back and specular reflection BC's. On a similar subject, Nie *et al.* [18] and Lim *et al.* [19] performed simulations of microsystems by relating the LBM relaxation time to the Knudsen number. According to Ref. [20], slip velocity relates directly to the relaxation time, and thus different relaxation times would certainly produce different degrees of slipping. On a theoretical ground, Ansumali and Karlin derived LBM BC's from the continuous kinetic theory to study the slip phenomena [21]. However, such approaches were not related directly to the solid-fluid interaction, which indeed plays a crucial role in determining the slipping behavior. Interestingly, we note a picture from MD simulations [10–12] where macroscopic slip can occur without any microscopic slip. It was found

that molecules near the solid wall may have no relative slipping movement to the surface, i.e., no molecular slip over the surface. In the region away from the surface, the velocity profile matches that predicted from classical fluid mechanics with slip BC's and changes rapidly in the wall vicinity, so as to reach the wall velocity as the distance goes to zero. Based on these results, we study here liquid slip near a solid-liquid interface by employing a bounce-back no-slip BC in a LBM. To incorporate solid-liquid interactions, we employ a mean-field free-energy LBM model recently proposed as it has been shown to represent a more realistic solid-fluid interaction [22].

According to the mean-field version of van der Waals' theory, the total free-energy function for a fluid system can be expressed as [23–27]

$$F = \int d\mathbf{r} \left\{ \psi(\rho(\mathbf{r})) + \rho(\mathbf{r})V(\mathbf{r}) + \frac{1}{2}\rho(\mathbf{r}) \int d\mathbf{r}' \phi_{ff}(\mathbf{r}' - \mathbf{r})[\rho(\mathbf{r}') - \rho(\mathbf{r})] \right\}, \quad (1)$$

where $\psi(\rho)$ is a local free energy with respect to the bulk phase of density ρ. The second term represents contribution of external potential energy $V(\mathbf{r})$ to the free-energy F. The third term is a nonlocal term taking into account the free-energy cost of variations in density; $\phi_{ff}(\mathbf{r}' - \mathbf{r})$ is the interaction potential between two fluid particles locating at $\mathbf{r}'$ and $\mathbf{r}$. These integrations are taken over the entire space. With this expression of free energy, we define [22] a nonlocal pressure as

$$P(\mathbf{r}) = \rho(\mathbf{r})\psi'(\rho(\mathbf{r})) - \psi(\rho(\mathbf{r})) + \frac{1}{2}\rho(\mathbf{r}) \int d\mathbf{r}' \phi_{ff}(\mathbf{r}' - \mathbf{r})[\rho(\mathbf{r}') - \rho(\mathbf{r})]. \quad (2)$$

For a bulk fluid with uniform density, the nonlocal integral term disappears and Eq. (2) reverts to the equation of state of the fluid.

Here, we describe the implementation of these results into a LBM algorithm. In general, after discretization in time and space, the lattice Boltzmann equation (LBE) with BGK collision term can be written as

---

*Author to whom correspondence should be addressed. FAX: (780) 492-2200; electronic address: daniel.y.kwok@ualberta.ca

$$f_i(\mathbf{x} + \mathbf{e}_i, \, t+1) - f_i(\mathbf{x},t) = -\frac{1}{\tau}[f_i(\mathbf{x},t) - f_i^{eq}(\mathbf{x},t)], \quad (3)$$

where the distribution function $f_i(\mathbf{x},t)$ denotes particle population moving in the direction of $\mathbf{e}_i$ at a lattice site $\mathbf{x}$ and at a time step t; τ is the relaxation time, and $f_i^{eq}(\mathbf{x},t)$ is a prescribed equilibrium distribution function of the local fluid density ρ and velocity $\mathbf{u}$ given by $\rho = \Sigma_i f_i$ and $\rho\mathbf{u} = \Sigma_i f_i \mathbf{e}_i$ [28]. However, if an external force $\mathbf{F}(\mathbf{x},t)$ exists, we can modify the above relation to reflect the momentum change as $\rho\mathbf{u} = \Sigma_i f_i \mathbf{e}_i + \tau\mathbf{F}$ and employ the $\mathbf{u}$ produced here to calculate the equilibrium distribution function f_i^{eq} [22]. Redefining the fluid momentum $\rho\mathbf{v}$ to be an average of the momentum before collision $\Sigma_i f_i \mathbf{e}_i$ and that after collision and following the Chapman-Enskog procedure, a NS equation with the equation of state

$$P = \frac{c^2(1-d_0)}{D}\rho + \Phi \quad (4)$$

can be obtained, where Φ is the potential energy field related to $\mathbf{F}$ by $\mathbf{F}(\mathbf{x},t) = -\boldsymbol{\nabla}\Phi(\mathbf{x},t)$. In order to obtain the NS equation with a pressure term similar to that given by Eq. (2), we set an artificial Φ as follows:

$$\Phi(\mathbf{x},t) = \rho(\mathbf{x})\psi'(\rho(\mathbf{x})) - \psi(\rho(\mathbf{x})) - \frac{c^2(1-d_0)}{D}\rho(\mathbf{x})$$

$$+ \frac{1}{2}\rho(\mathbf{x})\int d\mathbf{x}' \, \phi_{ff}(\mathbf{x}' - \mathbf{x})[\rho(\mathbf{x}') - \rho(\mathbf{x})]. \quad (5)$$

The above equations set up a complete LBM scheme with the mean-field free-energy function implemented. Unlike some other mean-field LBM approaches [29–31], the nonlocal free-energy term here is expressed as an integration rather than a density gradient through a square-gradient approximation; such a square-gradient approach is inadequate for the description of solid-fluid interfaces. The integration term employed here is more general and can be reduced to that of the square-gradient approximation when the local density varies slowly [23,24].

Following Refs. [22,31], we adopt a van der Waals fluid model to express the free-energy of bulk fluid as

$$\psi(\rho) = \rho kT \ln\frac{\rho}{1-b\rho} - a\rho^2, \quad (6)$$

where a and b are the van der Waals constants, k is the Boltzmann constant, and T is the absolute temperature. In a lattice grid, the interaction potential ϕ_{ff} can be reduced to a single number K [28],

$$\phi_{ff}(\mathbf{x}' - \mathbf{x}) = \begin{cases} K, & |\mathbf{x}' - \mathbf{x}| = 1 \\ 0, & |\mathbf{x}' - \mathbf{x}| \neq 1 \end{cases}, \quad (7)$$

which measures the interaction strength among the nearest neighboring particles. Thus the nonlocal integral term can be replaced by a summation over the neighbors of a site $\mathbf{x}$. The solid-fluid interaction is modeled as an exponentially decaying attractive force [23],
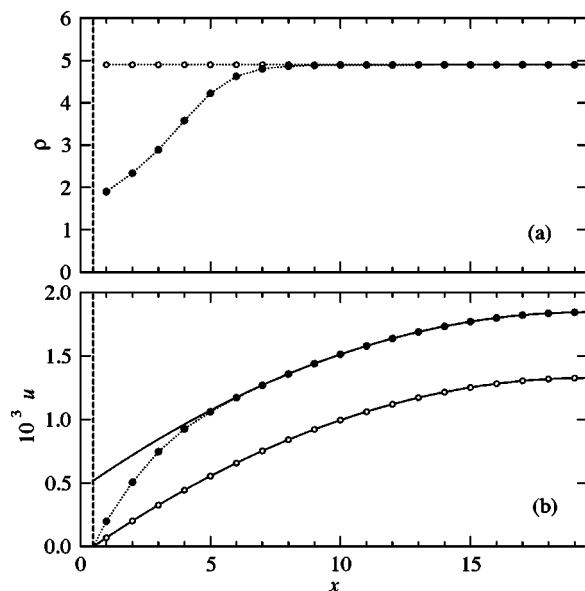
FIG. 1. (a) Density and (b) velocity profiles (half) calculated from a mean-field LBM (filled circles) and that in the limit of a standard no-slip Poiseuille flow (open circles). Solid lines in (b) are parabolic fittings using only the data points (for $x \geqslant 10$) away from the solid wall; the solid wall is represented by a dashed line at $x = 0.5$.

$$F_w(\mathbf{x}) = \rho(\mathbf{x})K_w e^{-h/\alpha}, \quad (8)$$

where K_w is the interaction strength, h is a distance from point $\mathbf{x}$ to the solid surface in lattice units, and α is a parameter controlling the decaying behavior. In our simulations, we selected $a = 9/49$, $b = 2/21$, and $kT = 0.55$. A 40×100 D2Q7 lattice domain for the slip simulations and a 128×256 D2Q7 domain for the contact angle simulations were employed with a relaxation time $\tau = 1$. The BC's applied to the top and bottom layer nodes are the general mid-grid bounce-back BC to simulate no-slip solid-fluid interfaces; periodic BC's were applied to the other two sides [14]. The fluid density in the slip simulations was set to be that of the liquid phase at equilibrium ($\rho_{bulk} = 4.895$).

Typical density and velocity profiles of pressure-driven Poiseuille flows are displayed in Fig. 1. The filled circles are simulation results from our mean-field LBM scheme with $K_w = 0$; for comparison purposes, we also illustrate the results from our mean-field model in the limit of a standard no-slip Poiseuille flow (i.e., $\Phi = 0$) as open circles. All other parameters in these two simulations remain the same. Because of symmetry, only half of the profiles are shown. As the wall is located at $x = 0.5$, the right boundary (at $x = 19.5$) corresponds to the channel center line. Unlike the constant density distribution (open circles) from the general LBM, there is a dry (low-density) layer between the bulk liquid and the wall (at $x = 0.5$) from our mean-field model (filled circles). Such a dry layer reflects the specific solid-fluid interactions in the vicinity of the wall. This result is similar to those obtained from thermodynamics [25] and observed in MD simulations [32]. However, because short-range interactions are neglected in this approximation, the density profile shows no oscillatory
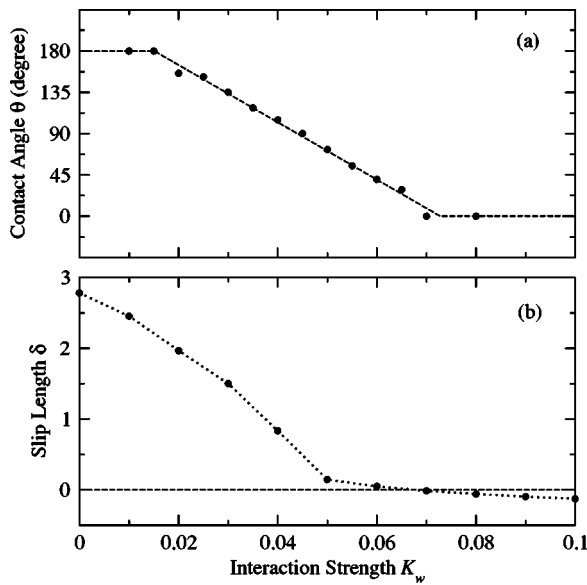
FIG. 2. Variation of (a) contact angle θ and (b) slip length δ with the solid-fluid interaction strength K_w.

FIG. 3. Variation of (a) contact angle θ and (b) slip length δ with the solid-fluid interaction decaying factor α where $\alpha = n\sqrt{3}/2$ for $n = 0.25$–2.75.

behavior near the wall as found from other MD studies [23,25].

In Fig. 1(b), the fluid velocity at the solid-fluid interface (at $x = 0.5$) is not directly available. Extrapolating the velocity data to this interface position results in a more or less zero velocity for both the mean-field LBM simulations and that in the limit of a standard no-slip Poiseuille flow. This demonstrates that the no-slip BC is satisfied and there is no microscopic slip at the solid-fluid interface. Thus the slip phenomenon discussed below does not appear to be a numerical artifact described elsewhere [20,33,34]. Comparing the two velocity profiles in Fig. 1(b), we found that the velocity from the mean-field LBM (solid circles) increases much faster in the dry layer ($1 \leq x \leq 6$); in the inner region (for $x \geq 7$), however, the variation of the two velocity profiles becomes similar. Through a parabolic fitting for the data points (for $x \geq 10$) in Fig. 1(b), we found that the velocity data from a general LBM follow the curve exactly; whereas, those from the mean-field LBM show good agreement only for $x \geq 6$ where the density is approximately constant. Extrapolating these fitted profiles to zero velocity yields a slip length δ, i.e., the distance between this zero velocity point and the wall; δ is positive if this zero-velocity point is outside the channel and negative if inside [10]. The slip lengths found in this specific example are 2.78 and 0 for the mean-field and general LBM, respectively. Overall, the velocity profile from the mean-field LBM model employed here is qualitatively similar to those obtained from MD simulations [10,11].

As a matter of fact, experimental and MD studies have shown that slip usually occurs on a hydrophobic surface. The origin of wettability and contact angle phenomena is, of course, from intermolecular interactions: the weaker the solid-fluid interaction, the more hydrophobic is the surface and hence the larger is the contact angle. For example, the choice of $K_w = 0$ in Fig. 1 should represent a low-energy (hydrophobic) surface. In Fig. 2, we plotted the contact angle θ and slip length δ values against the solid-fluid interaction
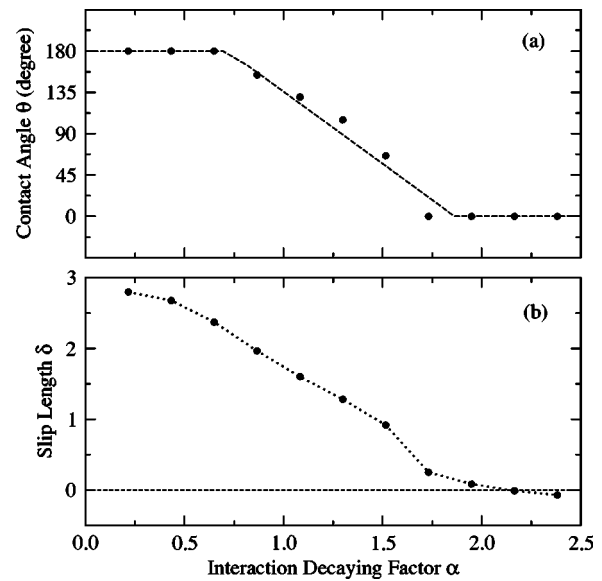
strength K_w with $\alpha = \sqrt{3}/2$. The contact angle is found to be nearly a linear function of K_w between $\theta = 0$ and 180° and is in agreement with those from other studies [32,35]. We point out that, unlike other multiphase LBM models, a contact angle value between 0 and 180° can be generated here without using a less realistic repulsive solid-fluid interaction. This is also consistent with physical reality and those observed in MD simulations [32].

In Fig. 2, as solid-fluid interaction increases, the slip length decreases quickly and becomes negative when $K_w > 0.06$. Beyond this value, the decrease in slip length becomes slower. Similar negative and small slip lengths had also been observed in MD simulations [10]. In fact, a positive slip length will produce a larger flow rate and can be considered as a wider channel [cf. Fig. 1(b)]; a negative slip length implies a smaller flow rate which corresponds to a narrower channel. The latter case appears to be possible when the solid-fluid interaction (adhesion) is very strong and molecules near the solid wall would have less mobility; the wall can then be thought of having an extra covered layer, resulting in a narrower channel. Focusing on the contact angle and slip length behaviors, we see that they follow similar decreasing trends as the solid-fluid attraction increases.

Another interesting factor that may influence the apparent slip length is the decaying behavior of the solid-fluid interaction in Eq. (8). Thus we plot in Fig. 3 the contact angle and slip length versus the variation of α, where $\alpha = n\sqrt{3}/2$ for $n = 0.25 - 2.75$. In this result, as α changes, the interaction strength K_w was adjusted to maintain the same value of F_w/ρ at $x = 1$; i.e., the first-layer fluid particles are set to experience the same body force from the wall. As α increases, the attractive force F_w in Eq. (8) will decay more slowly and thus can attract more fluid particles further away from the wall, resulting in a smaller contact angle and slip length. The phenomenon is similar to that shown in Fig. 2 and a small nega-

tive slip length is also observed. We have also studied the effects of the externally applied pressure on δ. However, unlike those from Refs. [12,17], our results suggest that slip length is independent of the magnitude of the driving force.

In summary, we have studied liquid slip over a solid surface with a no-slip boundary condition through a mean-field LBM. The resulting slip does not appear to be a numerical artifact. Our work relates interfacial slip to a more realistic solid-fluid interaction (and hence contact angle) directly. Results show that apparent macroscopic slip can occur even when there is no microscopic slip over the solid-fluid interface; its magnitude relates directly to the interaction strength between the fluid and solid particles. The results are in quali-tative agreement with those found from MD simulations. This study also demonstrates the kinetic nature of LBM when a more realistic solid-liquid interaction is considered. Obviously, liquid slip over a solid-fluid interface is a complex phenomenon where its physical principle remains unclear. With a better understanding of slip mechanism in the future, we believe that LBM could become a powerful alternative in these studies.

[1] G. Batchelor, *An Introduction to Fluid Dynamics* (Cambridge University Press, Cambridge, England, 1970).

[2] C. Navier, Memoirs de I'Academie Royale des Sciences de I'Institut de France **I**, 414 (1823).

[3] J. Maxwell, Philos. Trans. R. Soc. London **1** (1879), Appendix.

[4] N. Churaev, V. Sobolev, and A. Somov, J. Colloid Interface Sci. **97**, 574 (1984).

[5] D. Tretheway and C. Meinhart, Phys. Fluids **14**, L9 (2002).

[6] R. Pit, H. Hervet, and L. Leger, Phys. Rev. Lett. **85**, 980 (2000).

[7] V. S. J. Craig, C. Neto, and D. R. M. Williams, Phys. Rev. Lett. **87**, 054504 (2001).

[8] Y. Zhu and S. Granick, Phys. Rev. Lett. **88**, 106102 (2002).

[9] S. Gupta, H. Cochran, and P. Cummings, J. Chem. Phys. **107**, 10 316 (1997).

[10] M. Cieplak, J. Koplik, and J. R. Banavar, Phys. Rev. Lett. **86**, 803 (2001).

[11] M. Sun and C. Ebner, Phys. Rev. Lett. **69**, 3491 (1992).

[12] J.-L. Barrat and L. Bocquet, Phys. Rev. Lett. **82**, 4671 (1999).

[13] R. Benzi, S. Succi, and M. Vergassola, Phys. Rep. **222**, 145 (1992).

[14] S. Succi, *The Lattice Boltzmann Equation* (Oxford University Press, Oxford, 2001).

[15] S. Chen and G. D. Doolen, Annu. Rev. Fluid Mech. **30**, 329 (1998).

[16] B. Li and D. Y. Kwok, Phys. Rev. Lett. **90**, 124502 (2003).

[17] S. Succi, Phys. Rev. Lett. **89**, 064502 (2002).

[18] X. Nie, G. Doolen, and S. Chen, J. Stat. Phys. **107**, 279 (2002).

[19] C. Lim, C. Shu, D. Niu, and Y. Chew, Phys. Fluids **14**, 2299 (2002).

[20] X. He, Q. Zou, L.-S. Luo, and M. Dembo, J. Stat. Phys. **87**, 115 (1997).

[21] S. Ansumali and I. V. Karlin, Phys. Rev. E **66**, 026311 (2002).

[22] J. Zhang, B. Li, and D. Y. Kwok, Phys. Rev. E **69**, 032602 (2004).

[23] D. E. Sullivan, J. Chem. Phys. **74**, 2604 (1981).

[24] B. Widom, J. Stat. Phys. **19**, 563 (1978).

[25] A. E. van Giessen, D. J. Bukman, and B. Widom, J. Colloid Interface Sci. **192**, 257 (1997).

[26] J. Zhang and D. Y. Kwok, J. Phys. Chem. B **106**, 12 594 (2002).

[27] J. Zhang and D. Y. Kwok, Langmuir **19**, 4666 (2003).

[28] X. Shan and H. Chen, Phys. Rev. E **49**, 2941 (1994).

[29] L.-S. Luo, Phys. Rev. E **62**, 4982 (2000).

[30] X. He and G. D. Doolen, J. Stat. Phys. **107**, 309 (2002).

[31] M. R. Swift, E. Orlandini, W. R. Osborn, and J. M. Yeomans, Phys. Rev. E **54**, 5041 (1996).

[32] M. J. P. Nijmeijer, C. Bruin, A. F. Bakker, and J. M. J. van Leeuwen, Phys. Rev. A **42**, 6052 (1990).

[33] B. Li and D. Y. Kwok, Phys. Rev. Lett. **92**, 139402 (2004).

[34] L. S. Luo, Phys. Rev. Lett. **92**, 139401 (2004).

[35] Q. Kang, D. Zhang, and S. Chen, Phys. Fluids **14**, 3203 (2002).